Catalysis Communications 23 (2012) 20–24

Contents lists available at SciVerse ScienceDirect

Catalysis Communications

journal homepage: www.elsevier.com/locate/catcom

Short Communication

Synthesis of C_2-oxygenates from syngas over Rh-based catalyst supported on SiO_2, TiO_2 and SiO_2–TiO_2 mixed oxide

Lupeng Han, Dongsen Mao *, Jun Yu, Qiangsheng Guo, Guanzhong Lu

Research Institute of Applied Catalysis, School of Chemical and Environmental Engineering, Shanghai Institute of Technology, Shanghai 201418, P. R. China

ARTICLE INFO

Article history:
Received 4 January 2012
Received in revised form 26 February 2012
Accepted 29 February 2012
Available online 8 March 2012

Keywords:
Syngas
C_2 oxygenates
Rh-based catalysts
SiO_2–TiO_2 mixed oxide

ABSTRACT

SiO_2, TiO_2 and SiO_2–TiO_2 mixed oxide were synthesized by sol–gel method and used as supports for Rh-based catalysts. The effect of support on the performance of Rh-based catalysts for C_2-oxygenates synthesis from syngas was investigated by XRD, N_2 adsorption-desorption, FT-IR, H_2-TPD, H_2-TPR and TPSR techniques. The results indicated that SiO_2–TiO_2 supported catalyst had higher dispersion of Rh and thus more Rh^+ sites, better capability for CO adsorption and dissociation, and moderate ability for hydrogenation. As a result, SiO_2–TiO_2 supported Rh-based catalyst exhibited higher activity and C_2 oxygenates selectivity compared with counterparts supported on TiO_2 and SiO_2.

1. Introduction

It is well known that supported Rh-based catalysts exhibit excellent performances for the synthesis of C_2 oxygenates such as ethanol and acetaldehyde from hydrogenation of CO [1–4]. So far, quite extensive research on promoters and supports that contribute to higher activity and selectivity toward formation of C_2 oxygenates has been reported. For example, appropriate addition of promoters, such as Mn, Li, Fe, Ti, La, Sm, V, etc., could notably increase the activity and selectivity toward target products [5–11]. Previous work on supports has been concentrated principally on SiO_2 due to its high surface area, ample porosity and good stability [12–14]. On the other hand, it has been reported that Ti as a promoter or as a support both could promote the formation of C_2 oxygenates [6,8,15,16]. However, SiO_2–TiO_2 mixed oxide that may combine the advantages that SiO_2 is beneficial to the improvement of CO adsorption for its high surface area and TiO_2 may boost the formation of C_2 oxygenates has not been reported as support for Rh-based catalyst for the synthesis of C_2 oxygenates until to now, to the best of our knowledge.

In the present study, in order to illuminate the contribution to catalytic performance toward the formation of C_2 oxygenates that Rh-based catalyst supported on SiO_2–TiO_2 mixed oxide has made, three kinds of supports prepared by sol–gel method, i.e. SiO_2, TiO_2 and SiO_2–TiO_2 mixed oxide, were used as the supports for Rh-based catalysts promoted by Mn and Li, and the reaction behavior of all catalysts in C_2 oxygenates synthesis were tested for CO hydrogenation and characterized by X-ray powder diffraction (XRD), N_2 adsorption-desorption, Fourier transform infrared (FT-IR) spectroscopy, H_2 temperature-programmed desorption (H_2-TPD), H_2 temperature-programmed reduction (H_2-TPR) and temperature-programmed surface reaction (TPSR).

2. Experimental

2.1. Catalyst preparation

In order to eliminate the influence of the impurities in the supports [17], we here prepared the supports by sol–gel method using pure tetraethyl orthosilicate (TEOS) and tetrabutyl titanate (TBT) as the precursors of SiO_2 and TiO_2, respectively. The detailed procedures were as follows. (1) SiO_2. The mixed solution of 60 g TEOS (99.5%, SCRC) and 40 g anhydrous ethanol (99.7%, SCRC) was added slowly into the mixed solution of 4 g $NH_3 \cdot H_2O$ (26 vol.%, SCRC), 10 g H_2O and 40 g anhydrous ethanol under rapid stirring at 40 °C and reacted until the formation of white gel, which was then dried at 90 °C for 24 h. (2) TiO_2. The mixed solution of 17.4 g TBT (98.0%, SCRC) and 40 g anhydrous ethanol was added slowly into the mixed solution of 20 g acetic acid (99.5%, SCRC), 5 g H_2O and 40 g anhydrous ethanol under rapid stirring at 40 °C and reacted until the formation of yellow powder that was then dried at 90 °C for 24 h. (3) SiO_2–TiO_2 mixed oxide (the weight ratio of TiO_2:SiO_2 = 1:1). Firstly, the mixed solution of 3.5 g TEOS and 40 g anhydrous ethanol was added slowly into the mixed solution of 1.8 g $NH_3 \cdot H_2O$, 4 g H_2O and 40 g anhydrous ethanol under rapid stirring at 40 °C and reacted to the formation of sol. Secondly, the mixed solution of 4.3 g TBT and 40 g anhydrous ethanol was added slowly into the sol mixture and reacted until the formation

* Corresponding author. Tel.: +86 21 60877221; fax: +86 21 60877231.
E-mail address: dsmao@sit.edu.cn (D. Mao).

1566-7367/$ – see front matter © 2012 Elsevier B.V. All rights reserved.
doi:10.1016/j.catcom.2012.02.032

of white powder that was then dried at 90 °C for 24 h. All the supports were calcined in static air at 500 °C for 6 h before being used.

$RhCl_3$ hydrate (Rh ~36 wt.%, Fluka), $Mn(NO_3)_2$ solution (50%, SCRC), $LiNO_3$ (99.99%, SCRC) and supports mentioned above were used in catalyst preparations. All the catalysts were prepared by the incipient wetness impregnation method, and Rh loading were 2 wt.% and the weight ratio of Rh:Mn:Li = 2:1.5:0.07. Impregnated catalysts were dried at 90 °C for 8 h and subsequently calcined in static air at 350 °C for 4 h. The obtained catalysts are denoted as RML/SiO_2, RML/TiO_2 and RML/SiO_2–TiO_2, respectively.

2.2. Reaction

CO hydrogenation was performed in a fixed-bed micro-reactor with length ~350 mm and internal diameter ~5 mm. The catalyst (0.3 g) was loaded between quartz wool and axially centered in the reactor tube, with the temperature monitored by a thermocouple close to the catalyst bed. Prior to reaction, the catalyst was heated to 400 °C (heating rate ~3 °C/min) and reduced with H_2/N_2 (molar ratio of $H_2/N_2 = 1/9$, total flow rate = 50 mL/min) for 2 h at atmospheric pressure. The catalyst was then cooled down to 280 °C and the reaction started as gas flow was switched to a H_2/CO mixture (molar ratio of $H_2/CO = 2$, total flow rate = 50 mL/min) at 3 MPa. All post-reactor lines and valves were heated to 150 °C to prevent product condensation. The products were analyzed for both oxygenates and hydrocarbons on-line by Agilent GC 6820 equipped with a FID (flame ionization detector) and a TCD (thermal conductivity detector). The conversion of CO was calculated based on the fraction of CO that formed carbon-containing products according to: $\%\text{Conversion} = (\sum n_i M_i / M_{CO}) \cdot 100\%$, where n_i is the number of carbon atoms in product i, M_i is the percentage of product i detected, and M_{CO} is the percentage of CO in the syngas feed. The selectivity of a certain product was calculated based on carbon efficiency using the formula $n_i C_i / \sum n_i C_i$, where n_i and C_i are the carbon number and molar concentration of the ith product, respectively.

2.3. Catalyst characterization

XRD patterns were recorded on a PANalytical X'Pert instrument using Ni filtered Cu Kα radiation at 40 kV and 40 mA.

N_2 adsorption-desorption isotherms at −196 °C were obtained after outgassing of the sample under vacuum at 200 °C for 3 h, using a Micromeritics ASAP 2020M + C adsorption apparatus.

CO adsorption was studied using a Nicolet 6700 FT-IR spectrometer equipped with a DRIFT (diffuse reflectance infrared Fourier transform) cell with CaF_2 windows. The sample in the cell was pretreated in H_2/N_2 (molar ratio of $H_2/N_2 = 1/9$) at 400 °C for 2 h, and then the temperature was dropped to room temperature. After the cell was outgassed in vacuum to $<10^{-3}$ Pa, the background was scanned. Following by introducing CO into the IR cell ($p_{co} = 8.0 \times 10^3$ Pa), the IR spectrum of CO adsorbed on the catalyst was recorded. The concentration of CO was higher than 99.97%, and it was pretreated by dehydration and deoxygenization before being used. The spectral resolution was 4 cm^{-1} and the scan times were 64.

H_2 temperature-programmed desorption (TPD) was conducted by a flow gas chromatograph with TCD. 0.1 g of sample was reduced at 400 °C in H_2 for 1 h and cooled in H_2 to room temperature, then shifted into N_2. The adsorbed H_2 was desorbed in a flow N_2 of 50 mL/min and a heating rate of 10 °C/min.

H_2 temperature-programmed reduction (TPR) was carried out in a quartz microreactor. Firstly, 0.1 g of the as-prepared sample was pretreated at 350 °C in O_2/N_2 (molar ratio of $O_2/N_2 = 1/4$) for 1 h prior to a TPR measurement. During the TPR experiment, H_2/N_2 mixture was used at 50 mL/min and the temperature was ramped from room temperature to 500 °C at 10 °C/min while the effluent gas was analyzed with TCD.

The temperature-programmed surface reaction (TPSR) experiments were carried out as follows: after the catalyst was reduced at 400 °C in H_2/N_2 (molar ratio of $H_2/N_2 = 1/9$) for 2 h, it was cooled down to room temperature and CO was introduced for adsorption for 0.5 h; afterwards, the H_2/N_2 mixture was swept again, and the temperature was increased to 650 °C at the rate of 10 °C/min with a quadruple mass spectrometer as the detector to monitor the signal of CH_4 ($m/z = 15$).

3. Results and discussion

3.1. CO hydrogenation performances of the catalysts

Table 1 shows the performance of CO hydrogenation at 280 °C on all the catalysts. It was found that RML/TiO_2 showed the poorest catalytic performance with the lowest CO conversion and selectivity of C_2 oxygenates. Compared with RML/SiO_2, both higher CO conversion and C_2 oxygenates selectivity were obtained over RML/SiO_2–TiO_2, which indicated that SiO_2–TiO_2 mixed oxide as support can evidently improve the catalytic activity for the synthesis of C_2 oxygenates. The influence of SiO_2 and TiO_2 on CO hydrogenation over Rh catalyst was also investigated by other researchers [7,18]; however, their results suggested that Rh catalyst supported on TiO_2 was more active for syngas conversion and formation of C_2 oxygenates than that supported on SiO_2. The difference might be caused by the different structural and textural characteristics of the supports and the addition of Mn and Li in our catalysts.

3.2. XRD and N_2 adsorption results

Fig. 1 shows the XRD patterns of different catalysts. It can be seen that no diffractive signals of supported metals can be observed, indicating the high dispersion and small particle size of the supported metals. However, the possibility of the presence of the Rh_2O_3 phase on RML/TiO_2 cannot be completely ruled out, since the diffraction lines from Rh_2O_3 may overlapped with the strong TiO_2 lines [19]. On the other hand, the TiO_2 in the catalyst exists as pure anatase, while both SiO_2 and SiO_2–TiO_2 mixed oxide are X-ray amorphous. The result indicates that the addition of SiO_2 hinders the crystallization of amorphous TiO_2.

As shown in Table 2, SiO_2 supported catalyst has the biggest surface area, pore volume and pore diameter, but both CO conversion and C_2 oxygenates selectivity over it were lower than those over RML/SiO_2–TiO_2. Evidently, the textural characteristics of the catalysts were not directly related to their catalytic performances. This result is in line with those obtained by other researchers [20,21].

3.3. FT-IR study

Fig. 2 shows the IR spectra of the *in situ* reduced catalysts after CO adsorption at 30 °C for 30 min. As shown, bands characteristic of three typical adsorption states of CO could be observed on all the catalysts: geminal CO formed on the Rh^+ sites, with characteristic absorption band at ca. 2100 and 2030 cm^{-1}; linear CO on Rh^0 sites

Table 1
CO hydrogenation performance on different catalysts.

Catalyst	CO conversion (%)	Selectivity (%)						
		CO_2	CH_4	MeOH	HAc	EtOH	C_2^+H	C_2-oxy
RML/SiO_2	1.9	23.4	9.8	9.5	8.7	19.5	29.1	28.2
RML/TiO_2	1.4	27.8	10.0	8.5	7.7	14.9	31.0	22.6
RML/SiO_2–TiO_2	2.9	16.4	17.7	4.0	7.2	27.1	27.9	34.3

Reaction conditions: $t = 280$ °C, $p = 3$ MPa, $GHSV = 10000$ mL/(g·h), $V(H_2)/V(CO) = 2$. C_2^+H: Hydrocarbons containing two and more carbon atoms; C_2-oxy: Oxygenates containing two carbon atoms.

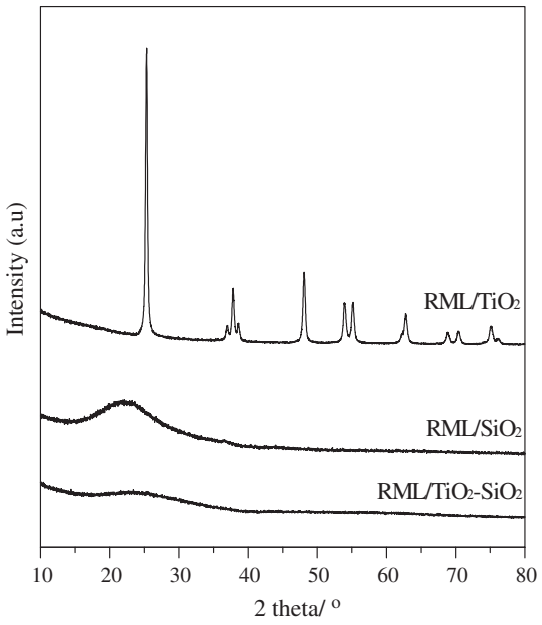

Fig. 1. XRD patterns of different catalysts.

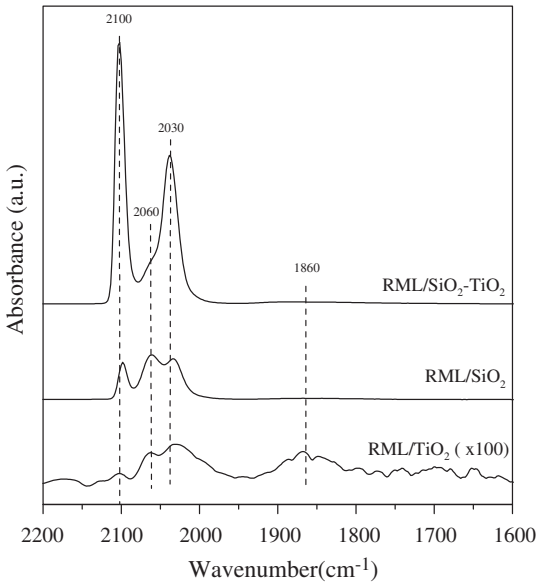

Fig. 2. IR spectra of CO chemisorbed on different catalysts at 30 °C for 30 min.

with absorption band at ca. 2060 cm^{-1} and bridged CO on Rh^0 sites with a broad absorption band at ca. 1860 cm^{-1} [13,22]. It can be seen from Fig. 2 that both the intensity of CO adsorption and the ratio of geminal CO/linear CO decreased in the order: RML/SiO_2–TiO_2 > RML/SiO_2 > RML/TiO_2, indicating that both the adsorption amount of CO and the ratio of Rh^+/Rh^0 sites decreased in the order: RML/SiO_2–TiO_2 > RML/SiO_2 > RML/TiO_2.

It has been suggested that the increment of gem-dicarbonyl CO adsorption implied increment of Rh dispersion [23], which could improve the selectivity toward C_2 oxygenates [15]. It is well acknowledged that Rh^0 is the active center for CO dissociation, and Rh^+ sites are responsible for CO insertion to form intermediates of C_2 oxygenates [24–26]. Thus, RML/SiO_2–TiO_2 owns more activity sites, especially the active sites for CO insertion. Based on the well-known C_2 oxygenates formation mechanism [27], excellent CO conversion and selectivity toward C_2 oxygenates were ineluctably obtained on RML/SiO_2–TiO_2, which also explained the poor catalytic performance on RML/TiO_2 for its deficient CO absorption.

3.4. H_2-TPD and H_2-TPR studies

H_2-TPD technique was also used to investigate Rh dispersion over different catalysts. As shown in Fig. 3, all the catalysts have two peaks of desorbed H_2 at about 100 and 500 °C, respectively. The high temperature peak is attributed to H_2 desorption from big Rh particles, while the lower temperature peak is attributed to H_2 desorption from more highly dispersed Rh particles [10]. It can be seen that the areas of both the two peaks decreased in the order: RML/SiO_2–TiO_2 > RML/SiO_2 > RML/TiO_2, which indicated that Rh dispersion decreased in the same order [18].

Fig. 4 shows the TPR profiles of the different catalysts. There were three peaks of H_2 consumption in the TPR profiles of all the catalysts below ca. 250 °C. According to the literature [28], the first two peaks were ascribed to the reduction of Rh_2O_3 not intimately contacting with Mn species (denoted as Rh I species) and of Rh_2O_3 intimately contacting with Mn species (denoted as Rh II species), respectively; and the third one was ascribed to the reduction of MnO_2. Furthermore, peaks above 250 °C on RML/TiO_2 and RML/SiO_2–TiO_2 might be attributed to partial reduction of TiO_2.

It can be seen, from Fig. 4, that the reduction temperatures of both Rh and Mn species increased in the order: RML/SiO_2–TiO_2 < RML/SiO_2 < RML/TiO_2. Based on the literature [21], the result indicated that the sizes of Rh and Mn oxide clusters increased in the order: RML/SiO_2–TiO_2 < RML/SiO_2 < RML/TiO_2, which implying that the Rh dispersion decreased in the order: RML/SiO_2–TiO_2 > RML/SiO_2 > RML/TiO_2. The result agreed with those from FT-IR and H_2-TPD studies, which can explain the order of the CO conversion and selectivity toward C_2 oxygenates over the different catalysts [15].

On the other hand, it is worthy to note that the intensity of the Rh II species on RML/SiO_2–TiO_2 was much weaker than those on the other two catalysts. This result indicated that the Rh–Mn interaction on RML/SiO_2–TiO_2 was the weakest. It is suggested that the catalytic

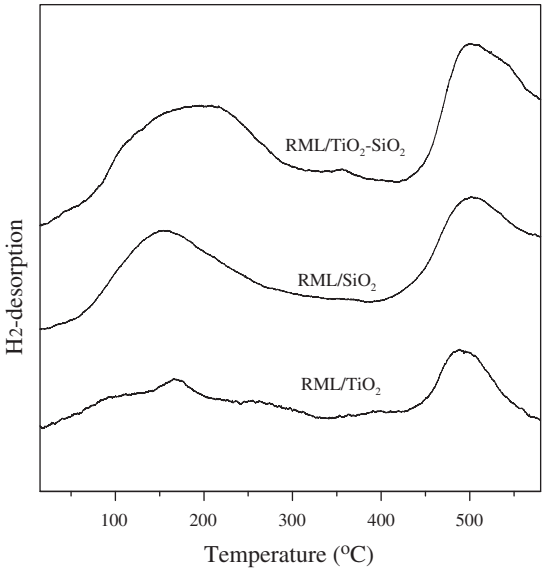

Fig. 3. H_2-TPD profiles of different catalysts.

Table 2
Textural characteristics of different catalysts.

Catalyst	S_{BET} (m^2/g)	Pore volume (cm^3/g)	Pore diameter (nm)
Rh–Mn–i/TiO_2	7.5	0.012	6.6
Rh–Mn–Li/SiO_2	98.6	0.378	11.3
Rh–Mn–Li/SiO_2–TiO_2	79.5	0.145	7.0

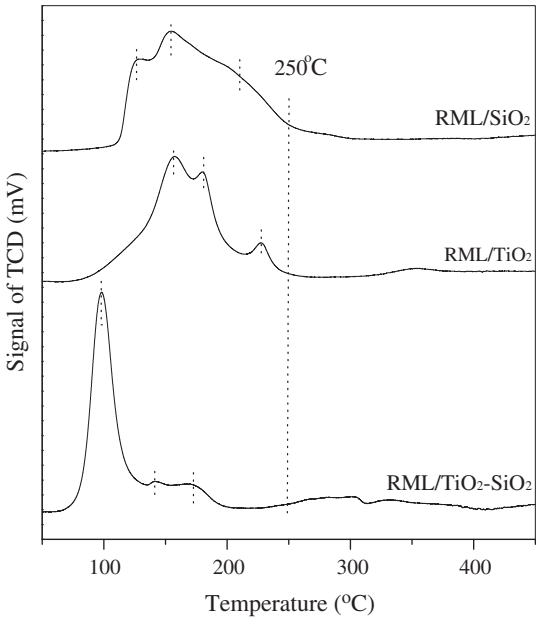

Fig. 4. H_2-TPR profiles of different catalysts.

property of Rh–Mn-based catalyst is very sensitive to the strength of Rh–Mn interaction [8,28]. In our case, the weakest Rh–Mn interaction corresponds to the highest activity for the synthesis of C_2 oxygenates. This result is in good agreement with that obtained by Chen et al. [28] who investigated the effect of Ti at low level on the catalytic performance of Ti promoted Rh–Mn–Li/SiO_2 for the synthesis of C_2 oxygenates.

3.5. TPSR study

As known that during the process of CO hydrogenation, the formation of CH_4 contains two procedures, that is CO dissociation to form CH_x species and then hydrogenation to form CH_4. Thus, the profile of CH_4 formation indirectly indicates the ability of CO dissociation related to the temperature of CH_4 formation and that of hydrogenation correlated with the peak intensity of CH_4 formation [21,29]. As shown in Fig. 5, CH_4 could be formed at the lowest temperature on RML/SiO_2–TiO_2 catalyst with the prime capability of CO dissociation, and the peak intensity of which remains mediocre with medium capability of hydrogenation. It has been found that there was a peak of CH_4 on RML/SiO_2–TiO_2 at ca. 600 °C, which might be attributed to the hydrogenation of carbon formed at lower temperatures and transformed to a less active form [30].

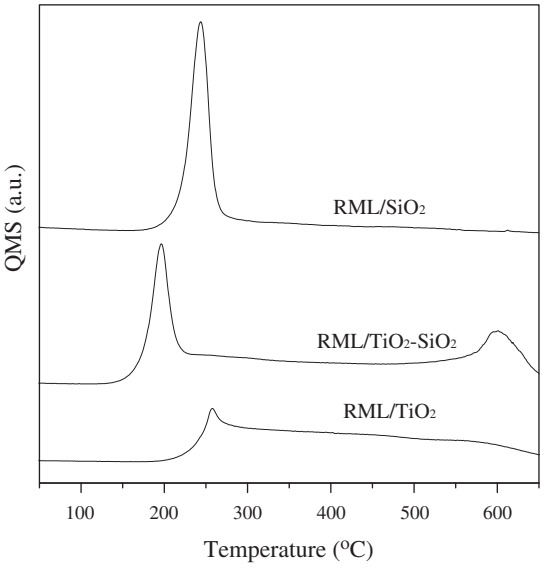

Fig. 5. TPSR profiles of different catalysts for CH_4 formation.

Chen et al. [31] argued that CO dissociation followed by hydrogenation into CH_x was interrelated with the activity of catalysts; moreover, CH_x hydrogenation into CH_4 and CH_x carbonylation as the precursor of C_2 oxygenates was a competing reaction. Therefore, high activity and selectivity of C_2 oxygenates were obtained on RML/SiO_2–TiO_2, for its excellent ability of CO dissociation and moderate ability of hydrogenation.

4. Conclusions

Compared with SiO_2 and TiO_2, Rh–Mn–Li catalyst supported on SiO_2–TiO_2 mixed oxide was more effective for the formation of C_2 oxygenates. Results from FT-IR and TPSR indicated that the significant increment of CO adsorption and excellent capability of CO dissociation were obtained on RML/TiO_2-SiO_2, which notably improved the catalytic activity. Results from FT-IR, H_2-TPD and H_2-TPR confirmed that SiO_2–TiO_2 mixed oxide improved the Rh dispersion and thus led to increment of Rh^+ sites, which improved the selectivity towards C_2 oxygenates. Moreover, moderate ability of hydrogenation was also conductive to increase the selectivity toward C_2 oxygenates.

Acknowledgments

The authors gratefully acknowledge financial support from the Science and Technology Commission of Shanghai Municipality (08520513600), Leading Academic Discipline Project of Shanghai Education Committee (J51503) and Shanghai Special Fund for Outstanding Young Teachers (yyy10083).

References

[1] R. Burch, M.I. Petch, Applied Catalysis A: General 88 (1992) 39–60.
[2] H.M. Yin, Y.J. Ding, H.Y. Luo, H.J. Zhu, D.P. He, J.M. Xiong, L.W. Lin, Applied Catalysis A: General 243 (2003) 155–164.
[3] R.P. Underwood, A.T. Bell, Journal of Catalysis 111 (1988) 325–335.
[4] T.P. Wilson, P.H. Kasai, P.C. Ellgen, Journal of Catalysis 69 (1981) 193–201.
[5] H.Y. Luo, P.Z. Lin, S.B. Xie, H.W. Zhou, C.H. Xu, S.Y. Huang, L.W. Lin, D.B. Liang, P.L. Yin, Q. Xin, Journal of Molecular Catalysis A: Chemical 122 (1997) 115–123.
[6] S.C. Chuang, J.G. Goodwin Jr., I. Wender, Journal of Catalysis 95 (1985) 435–446.
[7] M.A. Haider, M.R. Gogate, R.J. Davis, Journal of Catalysis 261 (2009) 9–16.
[8] W.M. Chen, Y.J. Ding, H.Y. Luo, L. Yan, T. Wang, Z.D. Pan, H.J. Zhu, Chinese Journal of Applied Chemistry 22 (2005) 470–474.
[9] R.P. Underwood, A.T. Bell, Journal of Catalysis 109 (1988) 61–75.
[10] H.Y. Luo, W. Zhang, H.W. Zhou, S.Y. Huang, P.Z. Lin, Y.J. Ding, L.W. Lin, Applied Catalysis A: General 214 (2001) 161–166.
[11] J. Gao, X.H. Mo, A.C.Y. Chien, W. Torres, J.G. Goodwin Jr., Journal of Catalysis 262 (2009) 119–126.
[12] W.M. Chen, Y.J. Ding, D.H. Jiang, Z.D. Pan, H.Y. Luo, Catalysis Letters 104 (2005) 177–180.
[13] D.H. Jiang, Y.J. Ding, Z.D. Pan, W.M. Chen, H.Y. Luo, Catalysis Letters 121 (2008) 241–246.
[14] X.H. Mo, J. Gao, N. Umnajkaseam, J.G. Goodwin Jr., Journal of Catalysis 267 (2009) 167–176.
[15] H. Arakawa, T. Fukushima, M. Ichikawa, S. Natsushita, K. Takeuchi, T. Matsuzaki, Y. Sugi, Chemistry Letters (1985) 881–884.
[16] A. Erdöhelyi, F. Solymosi, Journal of Catalysis 84 (1983) 446–460.
[17] L.E.Y. Nonneman, A.G.T.M. Bastein, V. Ponec, R. Burch, Applied Catalysis 62 (1990) L23–L28.
[18] T. Ioannides, X. Verykios, Journal of Catalysis 140 (1993) 353–369.
[19] C. Mateos-Pedrero, C. Cellier, P. Ruiz, Catalysis Today 117 (2006) 362–368.
[20] Z.L. Fan, W. Chen, X.L. Pan, X.H. Bao, Catalysis Today 147 (2009) 86–93.
[21] G.C. Chen, C.Y. Guo, X.H. Zhang, Z.J. Huang, G.Q. Yuan, Fuel Processing Technology 92 (2011) 456–461.
[22] A.C. Yang, C.W. Garland, The Journal of Physical Chemistry 61 (1957) 1504–1512.
[23] Y. Wang, Z. Song, D. Mang, H.Y. Luo, D.B. Liang, X.H. Bao, Chinese Journal of Catalysis 19 (1998) 533–537.
[24] P.R. Watson, G.A. Somorjai, Journal of Catalysis 72 (1981) 347–363.
[25] M. Kawai, M. Uda, M. Ichikawa, The Journal of Physical Chemistry 89 (1985) 1654–1656.

[26] S.S.C. Chuang, S.I. Pien, Journal of Catalysis 135 (1992) 618–634.
[27] M. Ichikawa, T. Fukushima, Journal of the Chemical Society, Chemical Communications 6 (1985) 321–323.
[28] W.M. Chen, Y.J. Ding, D.H. Jiang, Z.D. Pan, H.Y. Luo, Journal of Natural Gas Chemistry 14 (2005) 199–206.
[29] D.H. Jiang, Y.J. Ding, Z.D. Pan, X.M. Li, G.P. Jiao, J.W. Li, W.M. Chen, H.Y. Luo, Applied Catalysis A: General 331 (2007) 70–77.
[30] Y. Wang, H.Y. Luo, D.B. Liang, X.H. Bao, Journal of Catalysis 196 (2000) 46–55.
[31] W.M. Chen, Y.J. Ding, D.H. Jiang, G.P. Jiao, H.J. Zhu, Z.D. Pan, H.Y. Luo, Chinese Journal of Catalysis 27 (2006) 999–1004.